Int J Adv Manuf Technol (2010) 50:93–100
DOI 10.1007/s00170-009-2512-y

ORIGINAL ARTICLE

An optimization strategy based on a metamodel applied for the prediction of the initial blank shape in a deep drawing process

Abdessalem Chamekh · Souad BenRhaiem · Houda Khaterchi · Hedi BelHadjSalah · Ridha Hambli

Received: 13 July 2009 / Accepted: 30 December 2009 / Published online: 2 February 2010

Abstract The transformation of the sheet into a product without failure and excess of material in a deep drawing operation means that the initial blanks should be correctly designed. Therefore, the initial blank design is a critical step in deep drawing design procedure. Consequently, an easy approach for engineers in predicting the initial blank shape is necessary to reduce wastage in material and to overcome the large time consumed in the classical approaches. Thus, the aim of the present investigation is to propose an automatic procedure for the quick sheet metal forming optimization. In fact, a metamodel will be build based on artificial neural networks which will be coupled then with an optimization procedure in order to predict the initial blank shape in a rectangular cup deep drawing operation. The metamodel is built from the finite element simulations using ABAQUS commercial code. This procedure allows a significant reduce of the CPU time compared to classical optimization one. The results show that the desired shape is in good agreement with the one calculated using the optimized blank shape.

Keywords Metal forming · Shape optimization · FEM · ANN modeling · Inverse approach

A. Chamekh (✉) · S. BenRhaiem · H. Khaterchi · H. BelHadjSalah
Laboratoire de Génie Mécanique,
Ecole Nationale d'Ingénieurs de Monastir,
Avenue Ibn Eljazzard,
Monastir 5019, Tunisia
e-mail: chamakh_ab@yahoo.fr

R. Hambli
Institute PRISME–Polytech'Orléans,
8 Rue Léonard de Vinci Orléans,
45072 Cedex 2, France

1 Introduction

Metal forming process is a complex technology in which many problems are still in full explorations. The shape/process optimization shows great potential in helping engineers to solve efficiently some of these fundamentals problems. In most forming process designs, such as in the deep drawing of a car fender, the final geometry of the specimen to be formed is prescribed. Moreover, the forming process must be designed to ensure that, after deformation and springback, the blank will reach this prescribed shape. However, most direct numerical tools cannot predict perfectly the specimen's geometry after deformation due to springback, nonhomogeneous deformations, necking or flaws in appearance, etc. [1]. For this reason, an automatic design of the initial geometry of the specimen and/or the forming tool shape in order to provide the desired final geometry after forming process is very attractive for forming process designers.

The initial blank shape is one of the most important process parameter that has a direct impact on the quality of the finished part as well as on the cost of the formed part. Many blank design approaches were proposed to determine the optimal initial blank. Among them are slip-line field method proposed by Vogel and Lee [2], Kuwabara et al. [3], and Chen et al. [4]; geometric approach developed by Gerdeen et al. [5]; backward tracing proposed by Kim et al. [6]; ideal forming suggested by Chung and Richmond [7] and Park et al. [8]; finite element inverse strategy used by Lee et al. [9]; and inverse approach proposed and developed by Guo et al. [10]. In all these approaches, the finite element inverse approach seems to be very efficient and accurate.

As the number of control points needed to define the contour of the initial blank shape is large, it becomes more

difficult to find the optimum blank that satisfy the design specifications during the forming process in a short time [11]. In fact, Ponthot et al. [12] compare eight proposed classical optimization algorithms in terms of robustness, accuracy, and time consumption. These optimization methods are coupled with a finite element code. Based on statistics from 11 numerical applications, it appears from [12] that some methods exhibit both robustness and accuracy but not being faster. These methods are very efficient in some cases, but reasonably costly in every considered numerical application because the number of these finite element (FE) simulations increases as well as the number of the model parameters to be identified. Therefore, the use of approximation models to substitute the expensive FE simulations in the optimization loops is an efficient approach to avoid the computation barrier to the application of modern computer-aided design/computer-aided engineering tools in design optimization [13, 14]. A large number of approximation methods have been introduced such as the response surface method, the designs of experiments (DOE), and evolutionary and artificial methods [15–17]. Among them, the artificial neural networks (ANN) have attracted a growing interest in recent years [18, 19]. The focus of this paper is to develop an ANN metamodel based on the FE method (FEM) which will be coupled with an optimization procedure (Broyden-Fletcher-Goldfarb-Shanno (BFGS), Davidon-Fletcher-Powell (DFP),...) to determine the optimal shape of the initial blank in a deep drawing process. This method is developed and tested to show that it can be an economical solution in reducing computing time on one hand and to avoid additional operations on final shape of the industrial products on the other hand. A rectangular cup is considered for research purposes [20], and numerical tools such as ABAQUS [21] and POON (in-house neural networks code) were used to determine the optimal initial blank.

The optimization problem description and the general outlines of the proposed approach are presented in Section 2. In Section 3, the built of both design of experiments and metamodel is presented. The results and discussions of the optimal initial blank are presented in Section 4, followed by conclusions in Section 5.

2 Optimization problem statement

2.1 Problem description

The problem here is to find the adequate initial shape of the blank in the case of a rectangular deep drawing operation. The proposed optimization method involves an initial blank shape, which is iteratively trimmed according to the deep drawing simulations results, to achieve the final optimal blank shape. To reach the discounted goals, an objective function must be defined. This function must describe the error between the predicted deformed shape and the desired one in every loop of the proposed optimization procedure. Therefore, the contour of the blank has to be parameterized. Figure 1 illustrates the proposed blank shape which is discretized by seven control points (P_i, $i = 1, 2, \ldots, 7$).

As shown in Fig. 1, a geometrical shape error is introduced to define the geometrical deviation quantitatively. Therefore, the objective function is defined as the difference between the target and the deformed blank curve as in the following Eq. 1:

$$\varphi = \sqrt{\frac{1}{n}\sum_{i=1}^{n}\left(\left(x_i^{\mathrm{Pred}} - x_i^{\mathrm{des}}\right)^2 + \left(y_i^{\mathrm{Pred}} - y_i^{\mathrm{des}}\right)\right)^2} \tag{1}$$

where n is the number of the control point's positions. The $x_i^{\mathrm{Pred}}$and $y_i^{\mathrm{Pred}}$are the predicted coordinates of the control point i. The $x_i^{\mathrm{des}}$and y_i^{des} are the desired coordinates of the control point i.

2.2 Optimization approach

The problem of nonlinear optimization may be defined in the standard form as:

$$\begin{cases} \min \varphi(X),\ X = \{x_i, y_i);\ i = 1, 2, ..., 7\} \\ L \le X \le U. \end{cases} \tag{2}$$

X represents the vector of design variables which are the positions of the control points in the blank shape. L and U represent, respectively, the lower and upper geometrical bounds on every design variable.

Figure 2 illustrates the proposed blank shape optimization strategy.

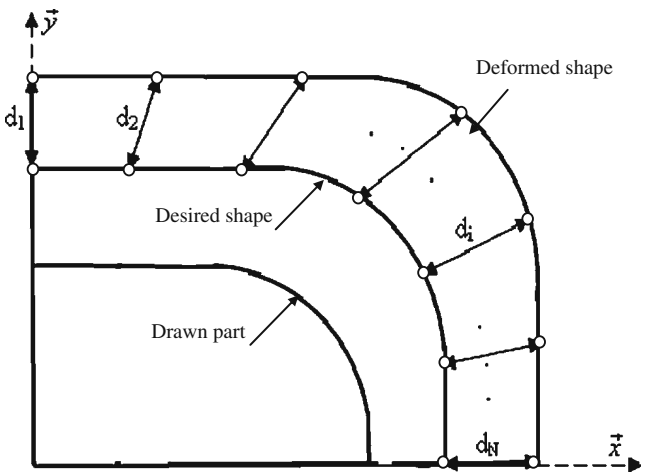

Fig. 1 Definition of the shape error

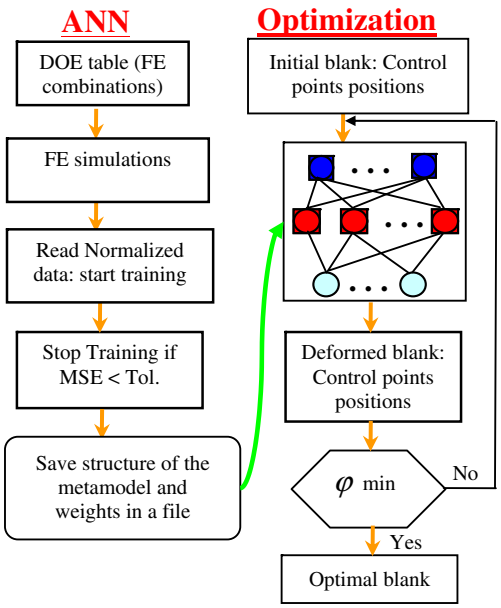

Fig. 2 Flowchart of proposed blank shape optimization approach

In the first stage, a DOE must be prepared based on the FE simulations of the rectangular deep drawing process. The DOE will be used then to build a metamodel based on a neural network technique. The input data are the control point positions for the initial blank, and the output parameters are the positions of the control points in the deformed configuration of the cup (Fig. 3).

Once validated, the metamodel will be coupled to the optimization algorithms (BFGS, DFP, and Levenberg–Marquardt).

This kind of intelligent method guarantees the rapidity of convergence. Moreover, the bounds of the design variables are constrained in a feasible region.

This optimization procedure was programmed under MATLAB software, and it is, then, coupled with process optimization neural networks, which are in-house neural network codes, developed by Chamekh et al. [22].

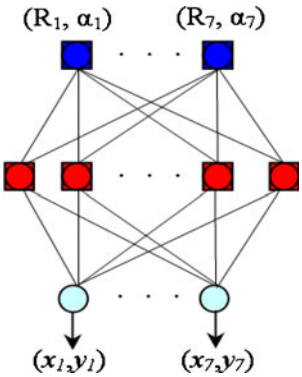

Fig. 3 Metamodel of the rectangular cup

3 Design of experiment

3.1 Finite element model

The finite element simulation of the deformed shape of the rectangular cup is made by using the ABAQUS commercial FEM code [21]. The deep drawing process is schematically drawn in Fig. 4. It illustrates the geometry and the dimensions of the tools used in the FE simulation of the rectangular cup. All dimensions are given in unit of millimeter.

Simulation of the deep drawing operation has been carried out for only one quarter of the rectangular cup due to the symmetry considering all the necessary process variables (Fig. 5). The die, the punch, and the blank holder are defined as discrete rigid bodies. The process is supposed to be quasi-static, and hence, the effects of strain rate are neglected.

The contour of the blank is described by a B-spline curve. Seven control points (P_1,..., P_7) are used to define the contour of the blank. The initial blank description is presented in Fig. 6. The p-degree B-spline curve C (t) in the t direction is defined as:

$$C(t) = \sum_{i=0}^{n} P_i N_{i,p}(t) \tag{3}$$

where:

$$N_{i,0}(t) = \begin{cases} 1 & \text{if } t_i \le t < t_{i+1} \\ 0 & \text{otherwise} \end{cases} \tag{4}$$

$$N_{i,p}(t) = \frac{t - t_i}{t_{i+1} - t_i} N_{i,p-1}(t) + \frac{t_{i+p+1} - t}{t_{i+p+1} - t_{i+1}} N_{i+1,p-1}(t) \tag{5}$$

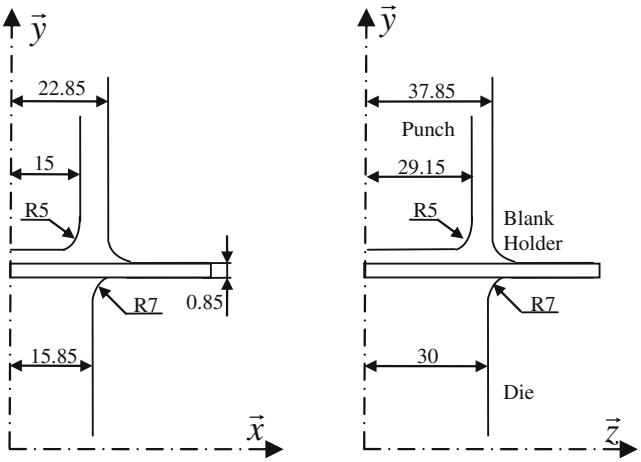

Fig. 4 Geometry and dimensions of the rectangular cup forming tools

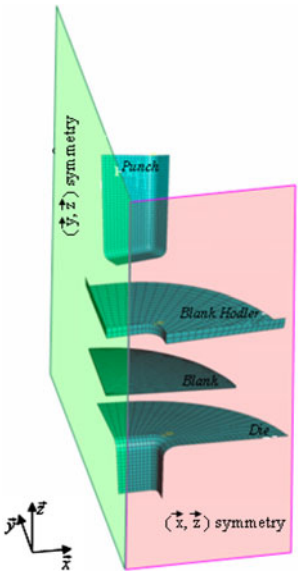

Fig. 5 Finite element model of the simulated process

$N_{i,p}(t)$ the normalized B-spline of degree p in the t direction

P_i the control point i

An AISI 304 stainless steel is used for this study. It has excellent corrosion resistance and good mechanical properties. Despite its high strength capabilities, it retains good formability characteristics compared to other high strength materials [23].

The material behavior model considered here is elastic–plastic formulated in a finite deformation assumption. The elastic behavior is assumed to be isotropic and is given by the Hooke's law. The considered plastic law is presented below:

The yield function is as follows:

$$f(\sigma,\alpha) = \sigma_c(\sigma) - \sigma_s(\alpha) \leq 0 \tag{6}$$

where σ_c is the equivalent stress, and σ_c (α) is the isotropic hardening function of the internal hardening variable α.

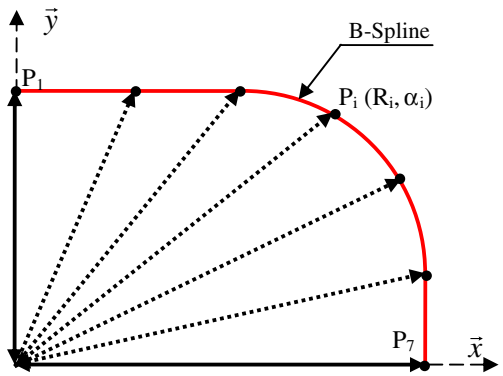

Fig. 6 Blank contour parameterization

The Hill's orthotropic yield criterion is considered here. In the case of the plane stress hypothesis, the yield stress function is, then, given as follows:

$$\sigma_c^2 = (G+H)\sigma_{11}^2 - 2H\sigma_{11}\sigma_{22} + (F+H)\sigma_{22}^2 + 2N\sigma_{12}^2 \tag{7}$$

where σ_{ij} represents the Cauchy stress components in the orthotropic axes; F, G, H, and N are the anisotropic coefficients of Hill in the plane stress state case. We introduce the condition $G+H=1$, so we have $\sigma_c=\sigma_{11}$ for the simple tensile test in the rolling direction.

The Lankford's coefficients are expressed versus the anisotropic coefficients as follows:

$$r_0 = \frac{H}{G};\ r_{90} = \frac{H}{F};\ r_{45} = \frac{2N-F-G}{2(F+G)} \tag{8}$$

Under the associative plasticity assumption, the plastic flow rule is given by relation 9:

$$D^p = \dot{\alpha}\frac{\partial f}{\partial \sigma}; \tag{9}$$

with $\dot{\alpha} \geq 0; \dot{\alpha} f = 0;\ \dot{\alpha}\dot{f} = 0$

The work hardening behavior is considered isotropic and is fitted according to the Swift power law:

$$\sigma = k(\varepsilon_0 + \varepsilon^p)^n \tag{10}$$

where σ is the equivalent stress, ε^p is the equivalent plastic strain, n and k are the hardening coefficients, and:

$$\varepsilon_0 = \left(\frac{\sigma_0}{k}\right)^{\frac{1}{n}} \tag{11}$$

Material properties are given in Table 1.

Initial process parameters were selected from empirical database. The blank holder force is 4.3 KN, and the friction coefficient between tools and blank is 0.25. These parameters are fixed through all the FE simulations. The die, the blank holder, and the punch were meshed by R3D4 element type. This mesh is produced with an average of element size of 1.2 mm. The blank, defined by parametric B-spline curve, is meshed by a S4R shell element type.

Table 1 Data for the blank material

Material properties	Value
E (GPa)	200
ν	0.33
ε_0	0.009
k (MPa)	1,330
n	0.35
r_0	1.24
r_{45}	0.99
r_{90}	1.2

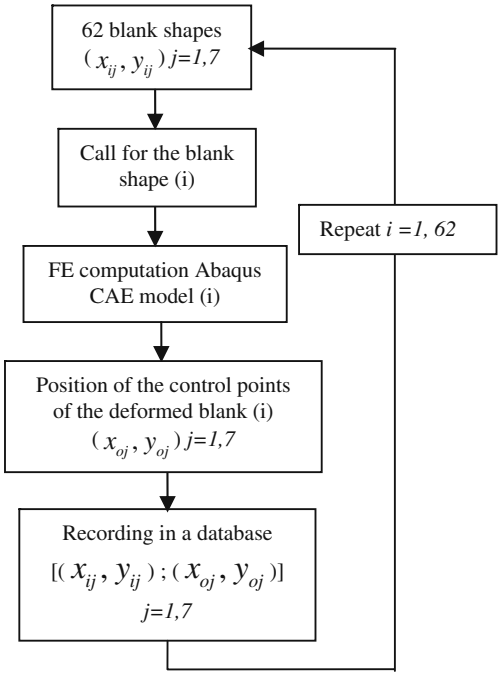

Fig. 7 DOE built procedure

3.2 DOE and ANN model

At the beginning, a DOE based on the finite element method is carried out. The flowchart of this DOE construction is presented in Fig. 7. If three levels for each control point are taken, the number of FE simulations will be 37=2,187 running. This number can be reduced by considering an optimal design of experiments called Box–Behnken design [24] to 62 FE running.

Once the DOE is built, the design variables and their corresponding responses are normalized between 0 and 1. Then, they are stored in a database which serves for the built of a process metamodel. Table 2 shows the level and the position values of each curve control point (Fig. 6).

Based on the established database, a multilayer perceptron is trained by backpropagation algorithm. This form of ANN can deal with nonlinear models with high accuracy. The input vector represents the control point's positions at the nondeformed blank shape, and the output vector represents the control point's positions at the deformed blank shape. Each neuron in the network operates by taking the sum of its weighted inputs ($W_{ij}O_i$) and passing the result through a nonlinear activation function (f). This is shown mathematically as:

$$O_i = f\left(\sum_j W_{ij}O_j + \theta_i\right) \tag{12}$$

The activation function used in this work is as follows:

$$f(x) = \frac{1}{1+e^{-\beta x}} \tag{13}$$

where β is a constant of convergence.

The network computes the weighted connections, minimizing the total mean squared error (Eq. 15) between the actual output of the network and the desired output. The weights are adjusted in the presence of momentum by:

$$\Delta_p W_{kj}(n) = \eta\delta_{pk}O_{pj} + \alpha\Delta_p W_{kj}(n-1) \tag{14}$$

where η is the gain term, δ_{pk} is an error term for node k, and α is a momentum term. The momentum term is added for fast convergence.

The major parameter used for evaluating the metamodel fitness during the training processes is the mean square error (MSE). This parameter is calculated as:

$$\mathrm{MSE} = \frac{1}{2}\sum_{j=1}^{P}\sum_{i=1}^{N}\left(t_{ij} - y_{ij}\right)^2 \tag{15}$$

where t_{ij} is the desired output, y_{ij} is the metamodel predicted response, P represents the total number of combinations in the training database, and N is the total number of the outputs.

In order to verify the accuracy and efficiency of the metamodel, an investigation in the training phase of the neural network (NN) model is conducted. For validation of the developed metamodel, we present in Fig. 8 the evolution of the MSE with respect to training repetitions.

As the number of training repetitions increases, the MSE decreases significantly. After 1,500 epochs, the MSE reach a value of 0.9%.

For more validation of the metamodel, three initial blank shapes are selected randomly (Fig. 9), which are not used during the training, and are simulated using the process

Table 2 Design variables and their bounds

Level	Parameters: R (mm), α (°)						
	R_1, α_1	R_2, α_2	R_3, α_3	R_4, α_4	R_5, α_5	R_6, α_6	R_7, α_7
1	30, 90	30, 75	35, 60	35, 45	45, 30	45, 15	45, 0
2	35, 90	35, 75	40, 60	40, 45	50, 30	50, 15	50, 0
3	40, 90	40, 75	45, 60	45, 45	55, 30	55, 15	55, 0

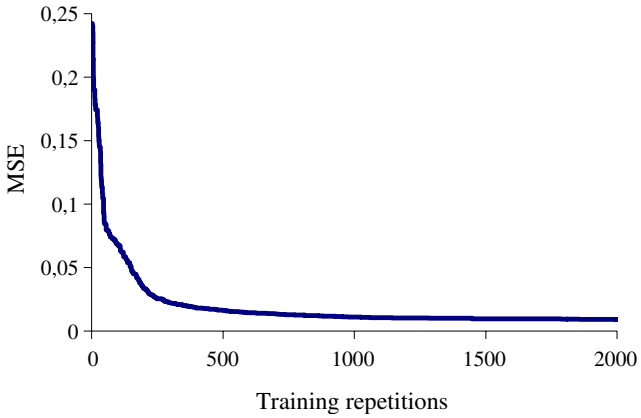

Fig. 8 The MSE evolution during the training phase

metamodel. They are compared with those calculated by the FE model.

As it can be shown from Fig. 10, the predicted blank shape obtained by the metamodel fits very well with the calculated one. The error between the two models is negligible. So, it can be concluded that the metamodel is capable of achieving the prediction of the deformed shape with high accuracy.

In order to verify the ability of the process metamodel in predicting the springback, the deformed blank relative to the first initial shape, obtained by the two models (FE and NN), is plotted in Fig. 11. The deformed shape predicted by the metamodel is compared to the one calculated by the FE model before and after the occurrence of the springback. The difference between the two deformed shapes means that the springback is handled. So, the metamodel incorporates elastic effect when predicts the deformed shape.

It is also noticed that the metamodel predicts the deformed shape in 1 s whereas the FE model takes 2 h to calculate the deformed shape on the same computation machine.

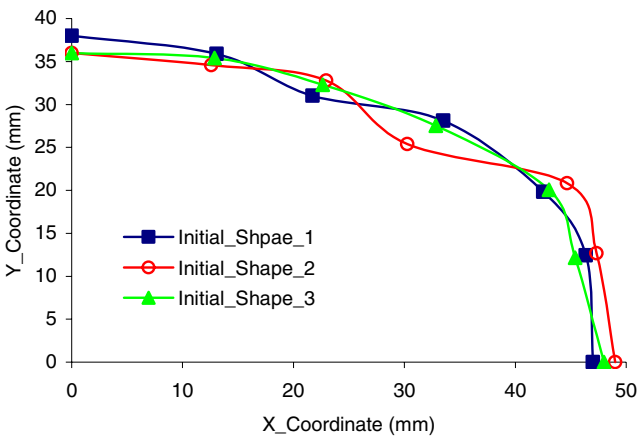

Fig. 9 Three initials shapes

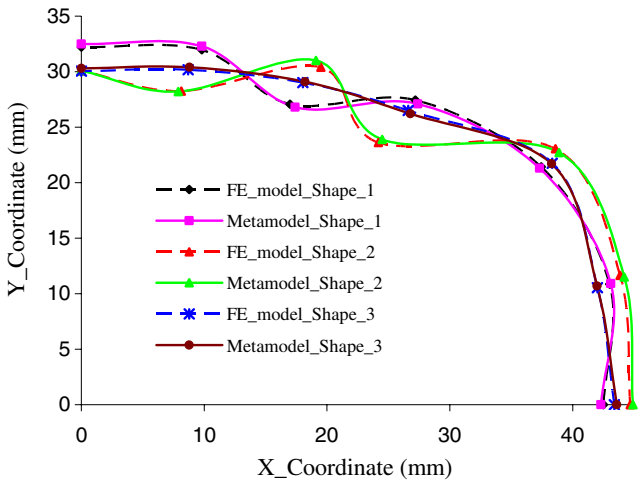

Fig. 10 Various final contour obtained by the metamodel and the FE model

4 Results and discussions

In order to find the optimal initial blank shape, the metamodel was coupled with the optimization procedure. In each optimization loop, the control point positions are predicted by the metamodel. Then, these positions will be compared to the desired positions in order to evaluate the objective function. This procedure is repeated until the convergence of the algorithm. Figure 12 shows the evolution of geometrical shape error over iterations for the three optimization method (BFGS, DFP, and Levenberg–Marquardt (LM)), which are coupled to the metamodel. As the number of iteration increases, the flange contour gets closer to the target contour. For the three cases, the error is reduced significantly, and the maximum shape error reaches a value of almost 0.2 mm. The whole optimization process needed 100 iterations for the BFGS and LM algorithms, and almost 60 iterations in the case of the DFP (Fig. 12). Although the

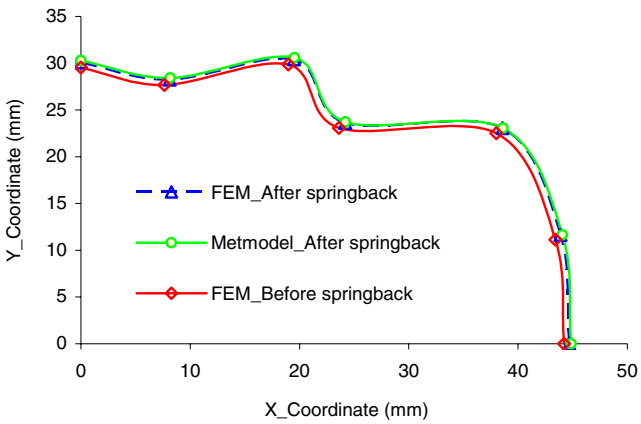

Fig. 11 Springback prediction

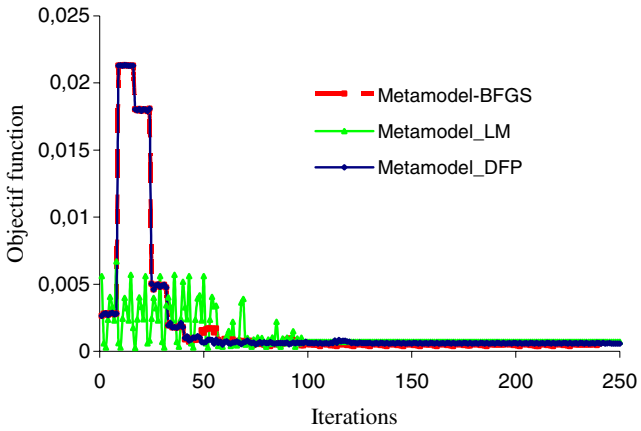

Fig. 12 Objective function evolution with respect to iteration number

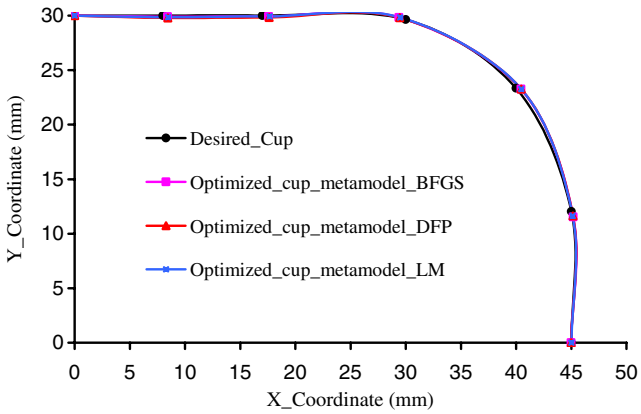

Fig. 14 Comparison between the desired final shape and the shape obtained by the optimal initial blank

number of iteration needed is so large, it is so clearly that the computing time consumed during the optimization processes is very fast since the CPU time needed during one iteration is almost equal to 1 s. Therefore, the whole optimization time did not exceed 6 min in the three cases in order to achieve the smallest error shape.

Figure 13 shows the optimal initial blank obtained by the proposed approach for the three cases. The initial blanks obtained by the three methods are close between them having almost the same form. It can be noted that these optimal blank shapes depend strongly on the choice of the friction coefficient, which is maintained here to an estimated experimental value of 0.25. In order to show the accuracy of the developed approach, the initial optimum blank shape obtained by each optimization method is used in a direct finite element simulation. The calculated deformed shape is compared to the desired one. These comparisons are presented in Fig. 14.

It appears from Fig. 14 that the FE deformed shapes are in good agreement with the prescribed final shape of the rectangular cup. The maximum error between the two shapes is equal to 0.2 mm.

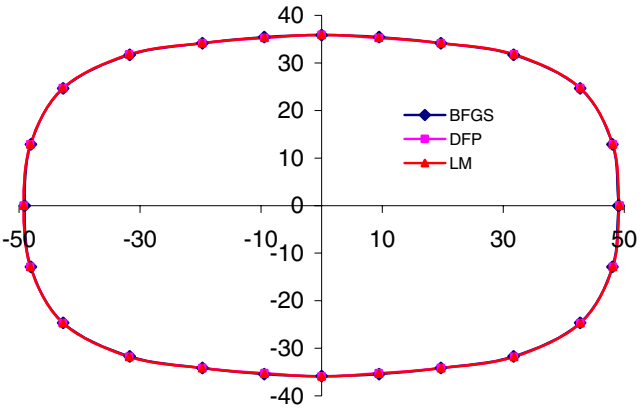

Fig. 13 The optimal initial shape of the blank obtained by different optimization algorithms

It is known that FE model coupled to gradient-based optimization algorithms is a CPU time consumer [12]. If we apply this method for multiparameters optimization, it can take much more CPU time. But once the metamodel is created and trained for this class of material law, and for this geometry, it is much faster than an FE computation and can be put into an optimization routine. In fact, the neural network approximates only the relevant dependencies for a parameter identification, which makes the metamodel smooth and better suitable for using inside a gradient-based optimization algorithm.

5 Conclusions

A sheet metal forming optimization based on metamodel was developed in this paper. It is applied on a deep drawing of a rectangular cup. It consists of the initial blank shape optimization taking in to account a priori knowledge of the workpiece. Firstly, a metamodel is built by combination of the ANN and FEM computations. Then, the metamodel is coupled to an optimization algorithm. The proposed method has the advantage that the time-consuming FE simulations are replaced by an ANN model in the optimization loops. However, if one wants to optimize another nonrectangular shape, or if the material model is varied, the ANN model has to be trained again, which is a disadvantage of the adopted approach. Although this drawback, the proposed approach remains a competitive tool compared to standard optimization methods. Moreover, the proposed procedure characterized by its simplicity and its rapidity has proved its robustness to provide an accurate solution. It appears to be very efficient in terms of precision despite of the highly nonlinear problems with multiparameter. The proposed approach can be widely used for the

design of very complicated blank geometry and can be applied for different optimization industrial problems.

References

1. Kleinermann JP, Ponthot JP (2003) Parameter identification and shape/process optimization in metal forming simulation. J Mater Process Technol 139:521–526
2. Vogel JH, Lee D (1990) An analytical method for deep drawing process design. Int J Mech Sci 32:891–907
3. TSi K (1997) PC-based blank design system for deep drawing irregularly shaped prismatic shells with arbitrarily shaped flange. J Mater Process Technol 63:89–94
4. Chen X, Sowarby R (1992) The development of ideal blank shapes by the method of plane stress characteristics. Int J Mech Sci 34:159–166
5. Gerdeen JC, Chen P (1989) Geometric mapping method of computer modelling of sheet metal forming. In Proc. Numiform Conf. Numerical Methods in Industrial Forming Processes. Balkema, Rotterdam, pp. 437–444
6. Kim SD, Park MH, Kim SJ, Seo DG (1998) Blank design and formability for non-circular deep drawing processes by the finite element method. J Mater Process Technol 75:94–99
7. Chung K, Richmond O (1992) Ideal forming II. Sheet forming with optimum deformation. Int J Mech Sci 34:617–633
8. Park SH, Yoon JW, Yang DY, Kim YH, Optimum blank design in sheet metal forming by the deformation path iteration method. Int J Mech Sci 41:1217–1232
9. Lee CH, Hub H (1998) Blank design and strain estimates for sheet metal forming processes by a finite element inverse approach with initial guess of linear deformation. J Mater Process Technol 1–3:145–155
10. Guo YQ, Batoz JL, Naceur H (2000) Recent developments on the analysis and optimum design of sheet metal forming parts using a simplified inverse approach. Comput Struct 78:133–148
11. Donglai W, Zhenshan C, Chen J (2008) Optimization and tolerance prediction of sheet metal forming process using response surface model. Comput Mater Sci 42:228–233
12. Ponthot JP, Kleinermann JP (2006) A cascade optimization methodology for automatic parameter identification and shape/process optimization in metal forming simulation. Comput Methods Appl Mech Eng 195:5472–5508
13. Se-Ho K (2002) BHF control algorithm with the design sensitivity analysis for the improvement of the deep drawn product. In Proc. Numisheet Conf. Jeju Island, Korea
14. Matthias H (1999) Optimization of sheet metal forming processes using simulation programs. In Proc. Numisheet Conf. Besancon, France
15. Subir R (2002) An automated and flexible approach to optimal design of shape and process variables for stamping parts. In Proc. Numisheet Conf. Jeju Island, Korea
16. Bahloul R, Ben-Elechi PA (2006) Optimization of springback predicted by experimental and numerical approach by using response surface methodology. J Mater Process Technol 173:101–110
17. Abendroth M, Kuna M (2006) Identification of ductile damage and fracture parameters from the small punch test using neural networks. Eng Fract Mech 73:710–725
18. Hambli R, Chamekh A, BelHadjSalah H (2006) Real-time deformation of structure using finite element and neural networks in virtual reality application. Finite Elem Anal Des 42:985–991
19. Chamekh A, BelHadjSalah H, Hambli R (2008) Inverse technique identification of material parameters using finite element and neural network computation. Int J Adv Manuf Technol. doi:10.1007/s00170-008-1809-6
20. Zhou D, Wagoner RH (1993) Development and application of sheet forming simulations. In Proceedings of the NUMISHEET'93 pp. 3–18
21. Abaqus (2001) Theory manual, standard user's manual and explicit user's manual, version 6.2, Hibbit, Karson & Sorensen, Inc
22. Chamekh A (2007) Optimisation de procédés de mise en forme par les réseaux de neurones artificiel. Thèse de doctorat en co-tutelle. ENIM/ISTIA, Tunisie
23. Padmanabhana R, Oliveira MC, Alvesb JL, Menezesa LF (2007) Influence of process parameters on the deep drawing of stainless steel. Finite Elem Anal Des 43:1062–1067
24. Aguir H, Chamekh A, BelHadjSalah H, Dogui A, Hambli R (2008) Identification of constitutive parameters using hybrid ANN multiobjective optimization procedure. Int J Mater Form. doi:10.1007/s12289-008-0008-1